Science of the Total Environment xxx (xxxx) 165891

Contents lists available at ScienceDirect

Science of the Total Environment

journal homepage: www.elsevier.com

Distinct variations in fluorescent DOM components along a trophic gradient in the lower Fox River-Green Bay as characterized using one-sample PARAFAC approach

Hui Lin [a, b], Sarah L. Bartlett [c], Laodong Guo [a, *]

[a] School of Freshwater Sciences, University of Wisconsin-Milwaukee, 600 E. Greenfield Ave., Milwaukee, WI 53204, USA
[b] Polar Research Institute of China, 1000 Xuelong Road, Pudong, Shanghai 201209, China.
[c] NEW Water/Green Bay Metropolitan Sewerage District, 2231 N. Quincy Street, Green Bay, WI 54302, USA

ARTICLE INFO

Editor: Shuzhen Zhang

Keywords:
Dissolved organic matter
Fluorescence EEM
Flow field-flow fractionation
Estuarine processes
Fox River-Green Bay
Lake Michigan

ABSTRACT

Variations in molecular weight distributions of dissolved organic matter (DOM) and PARAFAC-derived fluorescent components were investigated along a transect in the seasonally hypereutrophic lower Fox River-Green Bay using the one-sample PARAFAC approach coupling flow field-flow fractionation for size-separation with fluorescence excitation-emission matrix (EEM) and PARAFAC analysis. Concentrations of dissolved organic carbon and nitrogen, chromophoric-DOM, specific UV absorbance at 254 nm, and humification index all decreased monotonically from river to open bay, showing a strong river-dominated DOM source and a dynamic change in DOM quality along the river-lake transect. The relative abundance of colloidal DOM (>1 kDa) derived from ultrafiltration exhibited minimal variation, averaging 71 ± 4 % of the bulk DOM, across the entire estuarine transect although the colloidal concentration decreased in general. Using the one-sample EEM-PARAFAC approach, the identified major fluorescent components were distinct between stations along the river-estuary-open bay continuum, with four components in river/upper-estuary but three components in open bay waters. Among the four common fluorescent components (C_{475}, C_{410}, C_{320} and C_{290}), the most abundant and refractory humic-like component, C_{475}, behaved conservatively and its relative abundance (%ΣF_{max}) remained fairly constant (50 ± 4 %) along the transect, while the semi-labile humic-like component, C_{410}, consistently decreased from river to estuary and eventually vanished in open Green Bay. In contrast, the two autochthonous protein-like components (C_{320} and C_{290}) increased from river to open bay along the trophic gradient. The new results presented here provide an improved understanding of the diverse and fluctuating characteristics in DOM composition, lability, and estuarine mixing behavior across the river-lake interface and demonstrate the efficacy of the one-sample PARAFAC approach.

1. Introduction

Dissolved organic matter (DOM) plays an important role in regulating water quality, ecosystem dynamics, chemical speciation of trace elements, and biogeochemical processes in aquatic environments (Cole et al., 2007; Aiken et al., 2011; Lu et al., 2013). Over the past decades, fluorescence spectroscopy has been widely used since it provides information about DOM composition and sources in aquatic environments (Coble, 2007; Hudson et al., 2007; Fellman et al., 2010). When coupled with parallel factor analysis (PARAFAC), a statistical tool to deconvolute fluorescence (excitation-emission matrix, EEM) spectra into specific fluorescent components, EEM-PARAFAC delivers fingerprints information of DOM in different aquatic environments (Stedmon and Bro, 2008; Yang et al., 2015; Zhou et al., 2016a). However, PARAFAC analysis requires a relatively large sample size to establish a robust model (Stedmon et al., 2003; Murphy et al., 2013). Therefore, PARAFAC-derived fluorescent components are traditionally obtained from a combination of collective samples from different water depths and sampling locations, that may span diverse trophic, hydrological, or environmental gradients with different DOM sources and composition, especially at the river-lake and land-ocean interfaces (Osburn et al., 2015; Zhou et al., 2016b; Lee and Kim, 2018). To decipher changes in DOM composition between stations across a dynamic trophic, hydrological, or bio-

* Corresponding author.
E-mail address: guol@uwm.edu (L. Guo).

https://doi.org/10.1016/j.scitotenv.2023.165891
Received 6 June 2023; Received in revised form 27 July 2023; Accepted 27 July 2023
0048-9697/

geochemical interface, methods for EEM-PARAFAC analysis in single DOM samples are needed.

Wünsch et al. (2017) first introduced the one-sample PARAFAC approach that combines size exclusion chromatography and fluorescence spectroscopy. Lin and Guo (2020) also developed a similar one-sample PARAFAC approach coupling the flow field-flow fractionation (FlFFF) with EEM-PARAFAC analysis to characterize DOM size-distribution and fluorescent components for individual samples from different aquatic environments. However, applications of these newly developed methods have been rarely reported, especially for estuarine environments where changes in sources, composition and size spectra of DOM are extremely dramatic along transects from river to coastal waters (Stolpe et al., 2014; Zhou et al., 2016b; Xu et al., 2018a).

The lower Fox River-Green Bay system is the largest freshwater estuary in the world (Klump et al., 2009). Due to the dominance of nutrient and DOM input from the Fox-Wolf watershed, eutrophic conditions and seasonal hypoxia remain to be a persistent feature in the lower Green Bay (Bartlett et al., 2018; Klump et al., 2018). Indeed, there is a strong nutrient gradient in the lower Fox River-Green Bay ecosystem with hypereutrophic conditions in the upper estuary but oligotrophic in north Green Bay (DeVillbiss et al., 2016; Lin et al., 2016; Yang et al., 2021). Thus, the lower Fox River-Green Bay provides a natural laboratory to investigate variations in molecular size distribution and PARAFAC-derived fluorescent components of DOM from river to estuary to open bay waters using the one-sample PARAFAC approach.

Our hypothesis is that dynamic changes in water and environmental quality along the trophic gradient across the river-bay interface should result in distinguishable differences in PARAFAC-derived fluorescent DOM components between various stations within the lower Fox River-Green Bay ecosystem. One-sample EEM-PARAFAC analysis is thus an excellent approach for revealing the dynamic changes in fluorescent components across a gradient encompassing trophic, biogeochemical, and hydrological factors in aquatic environments. Our main objectives were 1) to examine the estuarine mixing behavior of chemical and optical properties of bulk DOM representing DOM quantity and quality, and 2) to assess changes in DOM fluorescent composition with molecular size both within individual samples and between different stations along the river-lake transect. We aimed to uncover the concealed changes in heterogeneous DOM across the trophic, hydrological, and biogeochemical interface.

2. Materials and methods

2.1. Study area

Green Bay is an arm of Lake Michigan (Fig. 1). The lower Fox River and the upper estuary of Green Bay was designated as one of the Areas of Concern (AOC) owing to extensive nutrient loadings and legacy organic pollutant input from the Fox River, which is the largest river draining into Green Bay. Even though nutrient inputs have been regulated for several decades in the United States including the Fox River-Green Bay system (Robertson et al., 2018), eutrophic conditions and seasonal hypoxia continued to be frequently observed in the study area (Bartlett et al., 2018; Klump et al., 2018). In addition to legacy nutrients and persistent organic pollutants, the Fox River also provides a major source of terrestrial DOM and emerging contaminants, including *per*- and polyfluorinated substances (PFAS), to Green Bay (DeVillbiss et al., 2016; Balgooyen and Remucal, 2022). Compared to freshwater discharge, the inflow from oligotrophic Lake Michigan is much higher than that from the Fox River (Modling and Beeton, 1970), resulting in a strong nutrient gradient from south (the upper estuary) to north (the lower estuary or open bay). In addition, this estuary has been characterized as a negative estuary, exhibiting high conductivity at the head of the estuary and lower conductivity in the open water areas (Xu et al., 2018a; Yang et al., 2021).

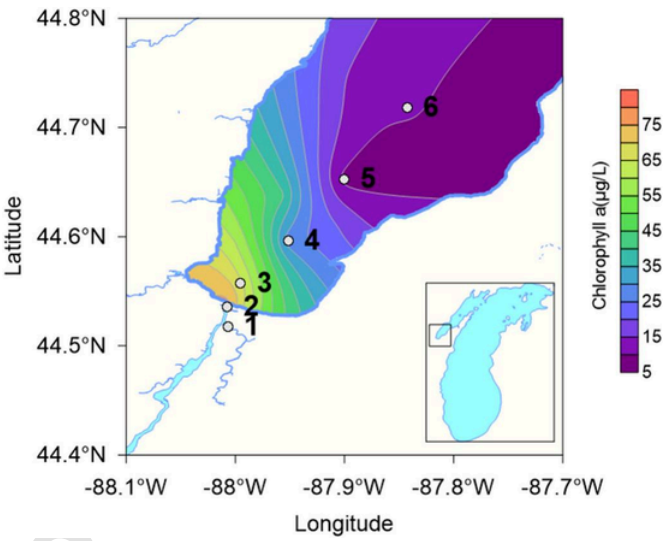

Fig. 1. Map showing the lower Fox River - Green Bay estuary, Lake Michigan, the sampling stations, and the distribution of surface water Chlorophyll *a* concentrations combining data from other stations.

2.2. Sample collection

Water samples were collected along a transect from the lower Fox River to open water in southern Green Bay during summer 2018 (Fig. 1). Station 1 was at the downstream of the East River, a tributary draining to Fox River main channel. Water temperature (°C), chlorophyll *a* concentration (μg/L) and specific conductivity (μS/cm) were obtained in situ using a multi-sensor probe (YSI Sonde).

Surface water samples were collected in acid-cleaned HDPE bottles and stored in a cooler filled with ice bags. Samples were filtered in the lab on the same day using pre-combusted (450 °C) GF/F membranes (0.7 μm, Whatman). Filtrates were collected in HDPE bottles (Nalgene) for the measurements of optical properties and in pre-combusted 20 ml glass vials for measurements of dissolved organic carbon (DOC) and total dissolved nitrogen (TDN). Samples were stored at 4 °C before pre-concentration for FlFFF analysis.

2.3. Measurements of DOC, TDN, and optical properties

Concentrations of DOC and TDN were measured on Shimadzu TOC-L analyzer with the high temperature combustion method (Guo and Santschi, 1997; Guo et al., 2012). Filtered water samples were acidified to pH < 2 before measurements of DOC. Analytical precision was within 2 % in terms of coefficient of variation. Ultrapure water, working standards, and consensus reference seawater samples from University of Miami were frequently measured as samples to check instrument performance and to ensure data quality. Concentrations of dissolved organic nitrogen (DON) were calculated from the difference between TDN and dissolved inorganic nitrogen (DIN), including nitrate, nitrite, and ammonium (Guo and Macdonald, 2006).

UV–visible absorption spectra (200–900 nm, 1 nm increments) were measured using a spectrophotometer (Agilent 8453) with a 10 mm quartz cuvette. Ultrapure water was used as a reference blank. UV-absorbance at 254 nm (A_{254}) was used to calculate the absorption coefficient at 254 nm (a_{254}, in m^{-1}, representing bulk CDOM) via $a_{254} = 2.303 \times A_{254}/l$, where l is the length of the cuvette (in meter). Spectral slope between 275 nm and 295 nm ($S_{275-295}$), a proxy for the molecular size of DOM, was calculated using non-linear regression to fit the absorbance spectra between 275 nm to 295 nm (Helms et al., 2008). Specific UV absorbance at 254 nm ($SUVA_{254}$, in L mg^{-1} m^{-1}), an indicator of aromaticity, was calculated as $SUVA_{254} = A_{254}/DOC$ (Weishaar et al., 2003). Absorbance ratio between 250 nm and 365 nm

(known as E2:E3 ratio) was used to track relative molecular size change (De Haan and De Boer, 1987), while the ratio of absorbance at 465 nm to 665 nm (known as E4:E6) was used as a CDOM aromaticity indicator (Summers et al., 1987; Piccolo et al., 1992).

Fluorescence EEM spectra were measured using a Horiba Fluoromax-4 spectrofluorometer with a 10 mm quartz cuvette, with excitation wavelengths varying from 250 to 480 nm (5 nm increment) and emission wavelengths scanned from 300 to 600 nm with 5 nm increment. Briefly, ultrapure water was used as a blank and scanned before sample measurements. The fluorescence intensities were calibrated into quinine sulfate equivalent (Q.S.E) using a series of quinine sulfate standard solutions (Zhou et al., 2016a). Biological index (BIX) and humification index (HIX) were calculated following published methods (Huguet et al., 2009; Lin et al., 2021).

2.4. Size-fractionation of DOM and FlFFF analysis

Prior to FlFFF analysis, water samples were first preconcentrated using stirred cell ultrafiltration (Amicon 8200) with a 1 kDa membrane (regenerated cellulose, YM1, Millipore). In addition, aliquots of the <0.7 μm filtrates were ultrafiltered to determine the abundance of the >1 kDa colloidal DOC and CDOM (in terms of a_{254}). The preconcentrated DOM samples were analyzed using an asymmetrical FlFFF system (Postnova, Salt Lake City, UT) for simultaneous online size separation and characterization (Zhou and Guo, 2015; Lin and Guo, 2020). The carrier solution is made of 10 mM NaCl, 5 mM H_3BO_3, and adjusted to pH = 8. The FlFFF system was coupled online with detectors, including a UV-absorbance detector (SPD-20A, Shimadzu, Japan), targeting at 254 nm absorbance representing bulk CDOM, and two fluorescence detectors (RF-20A, Shimadzu, Japan), measuring Ex/Em at 350/450 nm ($Fluor_{350/450}$) for humic-like DOM (Peak C) and 275/340 nm ($Fluor_{275/340}$) for protein-like DOM (Peak T), respectively.

2.5. EEM-PARAFAC analysis

Size-fractionated sub-samples were collected after the online detectors for further EEM measurements. The drEEM toolbox (v.0.5.0) was used to perform PARAFAC analysis on the Matlab (R2018b) platform (Murphy et al., 2013). PARAFAC analysis was performed on EEM data of size-fractionated samples from each individual sample. Therefore, the one-sample PARAFAC analysis developed unique PARAFAC models for each sample or station rather than for all stations (Lin and Guo, 2020). Non-negativity constraints were applied to established models in order to guarantee all positive values (Stedmon and Bro, 2008). Number of components was evaluated and determined by sum of squared errors. Tucker's congruence coefficient (TCC) was used in both the half-split validation and in comparisons and identification of components between models. To guarantee the reliability of our models, the threshold of TCC in the half-split validation was set at 0.95, but the TCC was set at 0.90 in the inter-model comparisons.

3. Results

3.1. Characterization of bulk DOM

Concentrations of DOC ranged from 441 μmol L^{-1} to 869 μmol L^{-1}, and values of a_{254} (or bulk CDOM) ranged from 27.7 m^{-1} to 64.2 m^{-1}. Specific conductivity decreased from 463 μS/cm (salinity 0.30) at the river water station to 322 μS/cm (salinity 0.20) in open bay waters during the sampling time period, showing the feature of a negative estuary (Xu et al., 2018a). Along with the declining specific conductivity, both DOC and CDOM also decreased from the lower Fox River to open Green Bay (Fig. 2), except the tributary sample that was collected away from the main river channel. The aromaticity indicators (both $SUVA_{254}$ and E4:E6) and humification index (HIX) also decreased consistently from the river to the bay, while both E2:E3 and $S_{275–295}$, indicators of DOM apparent molecular size, showed an opposite pattern (Fig. 2). Although the Chlorophyll *a* concentration at river mouth was nine time higher than those observed in open Green Bay (Fig. 1), values of biological index (BIX) showed an asynchronous pattern or increased gradually from river mouth to open bay water, indicating a more complex relationship between Chl-a and biogenic DOM. Similar to DOC and CDOM, concentrations of DON also decreased from river to open bay, with high DON at the tributary station, while DOC/DON ratios increased from river to open bay water (Fig. 2). Elevated DON concentration and low DOC/DON ratio at the river station suggested a main terrestrial DON source from the Fox River basin. In addition, different variation patterns in DOM and optical properties indicated that, although bulk DOM had a conservative mixing behavior, source and chemical properties of DOM evidently changed along the river-bay transect. For example, the terrestrial DOM was dominant in the Fox River and become progressively diluted in Green Bay, resulting in a rise in the proportion of fresh algal-derived DOM from the Fox River to Green Bay. This observation is consistent with the increasing trend in BIX along the river-bay transect (Fig. 2).

3.2. Molecular weight distributions of DOM

Colloidal DOC (>1 kDa) was 66 % - 77 % of the bulk DOC with an average of 71 ± 4 %, while colloidal CDOM was 65 % to 78 % of bulk CDOM a_{254} with an average of 73 ± 5 % (Fig. S1). Both colloidal DOC and CDOM abundances remained relatively constant along the river-bay transect, 71 ± 4 % and 73 ± 5 %, respectively. High abundances of colloidal DOC and CDOM have been widely reported for river waters and other freshwater environments (Belzile and Guo, 2006; Zou et al., 2006; Zhao et al., 2021). However, little changes in colloidal DOM abundance in this negative estuary with higher conductivity in river water are in contrast to those observed in marine estuaries where colloidal DOM significantly decreases from river water to seawater (Wen et al., 1999; Guo et al., 2009). In addition, the percentage of colloidal DOC here is significantly higher than those reported previously (e.g., Xu et al., 2018a; Zhao et al., 2021) due to the difference in membrane cutoffs and manufacturers or types of ultrafiltration device (centrifugal vs. disk membrane). As reported in Xu and Guo (2017), the actual membrane cutoff of a manufacture-rated 1 kDa membrane in a centrifugal ultrafiltration unit can be as high as 2.5 kDa. Thus, certain ultrafiltration devices might significantly underestimate the colloidal fraction ($>$ 1 kDa) of DOM since the most abundant DOM component, humic-like DOM, is largely in the 1–3 kDa size-fraction in natural waters (Lin and Guo, 2020; Li et al., 2023). Moreover, different sampling seasons might be another factor for the difference in colloidal DOC abundances.

Size spectra derived from FlFFF analysis showed that both UV_{254} (bulk CDOM, Fig. S2) and $Fluor_{350/450}$ (humic-like, Fig. S3) exhibited fractograms with a single-narrow-peak, while $Fluor_{275/340}$ (protein-like, Fig. S4) had a shoulder extending from the main peak towards larger molecular size regions. In general, $Fluor_{275/340}$ (protein-like fluorescent DOM) dominated in the 100 kDa –0.7 μm size-fraction (Fig. S4), while UV_{254} and $Fluor_{350/450}$ (humic-like) were mostly partitioned in the lower molecular weight fractions, including the 1–3 kDa and 3–10 kDa (Figs. S2 and S3). Similar distinct size-distributions between protein-like and humic-like components have been observed in various other aquatic environments (Stolpe et al., 2014; Wünsch et al., 2018; Lin and Guo, 2020).

To facilitate comparisons with those reported in previous studies, the FlFFF-divided size fractions were further integrated into four major size-fractions, including the 0.3–1 kDa, 1–3 kDa, 3–10 kDa, and $>$ 10 kDa (Fig. 3). Within the four DOM size-fractions, the 3–10 kDa was the dominated UV_{254} size-fraction, followed by the 1–3 kDa and $>$ 10 kDa size-fractions, while the 0.3–1 kDa was the least size-fraction. For the humic-like $Fluor_{350/450}$, the dominant size

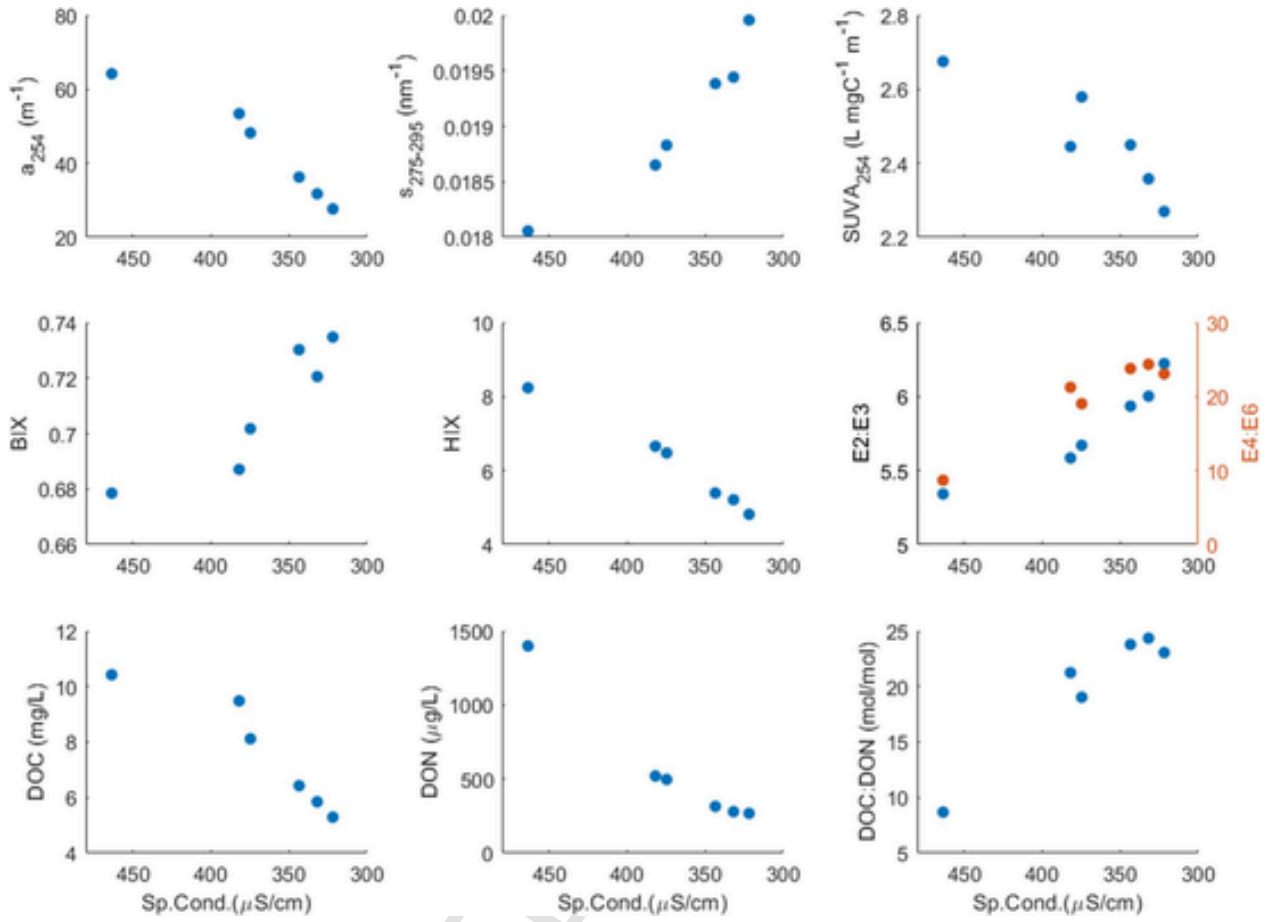

Fig. 2. Variations of UV absorption coefficient at 254 nm (a_{254}), spectral slope between 275 and 295 nm ($S_{275–295}$), specific UV absorbance at 254 nm ($SUVA_{254}$), biological index (BIX), E2:E3 and E4:E6 ratios, humification index (HIX), dissolved organic carbon (DOC), dissolved organic nitrogen (DON), and DOC/DON ratio with specific conductivity in the lower Fox River-Green Bay.

fractions included the 1–3 kDa and 3–10 kDa, followed by the > 10 kDa and then the 0.3–1 kDa. In contrast to both UV_{254} and $Fluor_{350/450}$, the >10 kDa was the most abundant $Fluor_{275/340}$ (or protein-like) size-fraction (> 60 %, Fig. S5), and the other three size-fractions had similar abundances although the 1–3 kDa and 3–10 kDa had a relatively higher abundance than the 0.3–1 kDa size-fraction (Fig. 3). In general, both UV_{254} and $Fluor_{350/450}$ (or humic-like) DOM had a more even size distribution, while $Fluor_{275/340}$ (or protein-like) DOM was mostly partitioned in the >10 kDa HMW size fraction.

Overall, higher abundances of bulk CDOM (UV_{254}) and humic-like ($Fluor_{350/450}$) DOM in all size fractions in the lower Fox River and monotonic decrease from river water (high conductivity) to open bay water (lower conductivity) attested to a dominant river source of both UV_{254} and $Fluor_{350/450}$. In contrast to bulk CDOM and humic-like DOM, the protein-like $Fluor_{275/340}$ in all size-fractions contained mostly HMW components in the >10 kDa size-fraction. Similarly low abundances were observed in other size-fractions of $Fluor_{275/340}$ without a clear variation trend along the river-bay transect (Fig. 3c). These indicated mostly an in-situ source of protein-like $Fluor_{275/340}$ from autochthonous processes in the water column (Cuss and Guéguen, 2015) and the effect of photochemical degradation on humic-like DOM (Chen and Jaffé, 2014; Xu et al., 2018c) especially in open waters.

3.3. Fluorescent components at each station derived from one-sample PARAFAC approach

Using the one-sample PARAFAC approach combining FlFFF size-separation and EEM-PARAFAC analysis (Lin and Guo, 2020), the PARAFAC-derived fluorescent components were acquired for each sampling station in the dynamic estuarine environment (Fig. 4). Although the EEM contours of bulk water samples were highly seemingly similar between each station (Fig. S6) in this river-dominated or terrestrial DOM-dominated estuarine system, the one-sample PARAFAC-derived fluorescent components are apparently different among sampling stations within the lower Fox River-Green Bay ecosystem (Fig. 4). For example, four major fluorescent components (including C_{475}, C_{410}, C_{320} and C_{290}) were identified for stations in the lower Fox River and upper estuarine region, but only a three-component model (with C_{475}, C_{320} and C_{290}) could be validated for station 6 from open Green Bay (Fig. 4).

In addition, among those stations with four major fluorescent components derived from the one sample PARAFAC approach (stations 1–5, Fig. 4), the relative importance of the four major fluorescent components was evidently different. For instance, they followed the order of $C_{475} > C_{320} > C_{410} > C_{290}$ at stations 1, 4 and 5, but $C_{475} > C_{320} > C_{290} > C_{410}$ at station 2 and $C_{475} > C_{410} > C_{320} > C_{290}$ at station 3. At the open bay station (station 6), one of the major fluorescent components, a humic-like fluorescent component (C_{410}), was depleted or vanished although the most abundant humic-like component (C_{475}) persisted, showing different lability between humic-like fluorescent components during estuarine mixing and a composition change in the bulk DOM pool across the river-lake interface.

To compare these fluorescent components among stations (Fig. 4), inter-modal comparisons were performed using TCC method to identify common major components (Table S1). Four major fluorescent components, including C_{475}, C_{320}, C_{410} and C_{290}, named after their characteristic emission maximum in their loadings (Fig. 5), were identified from

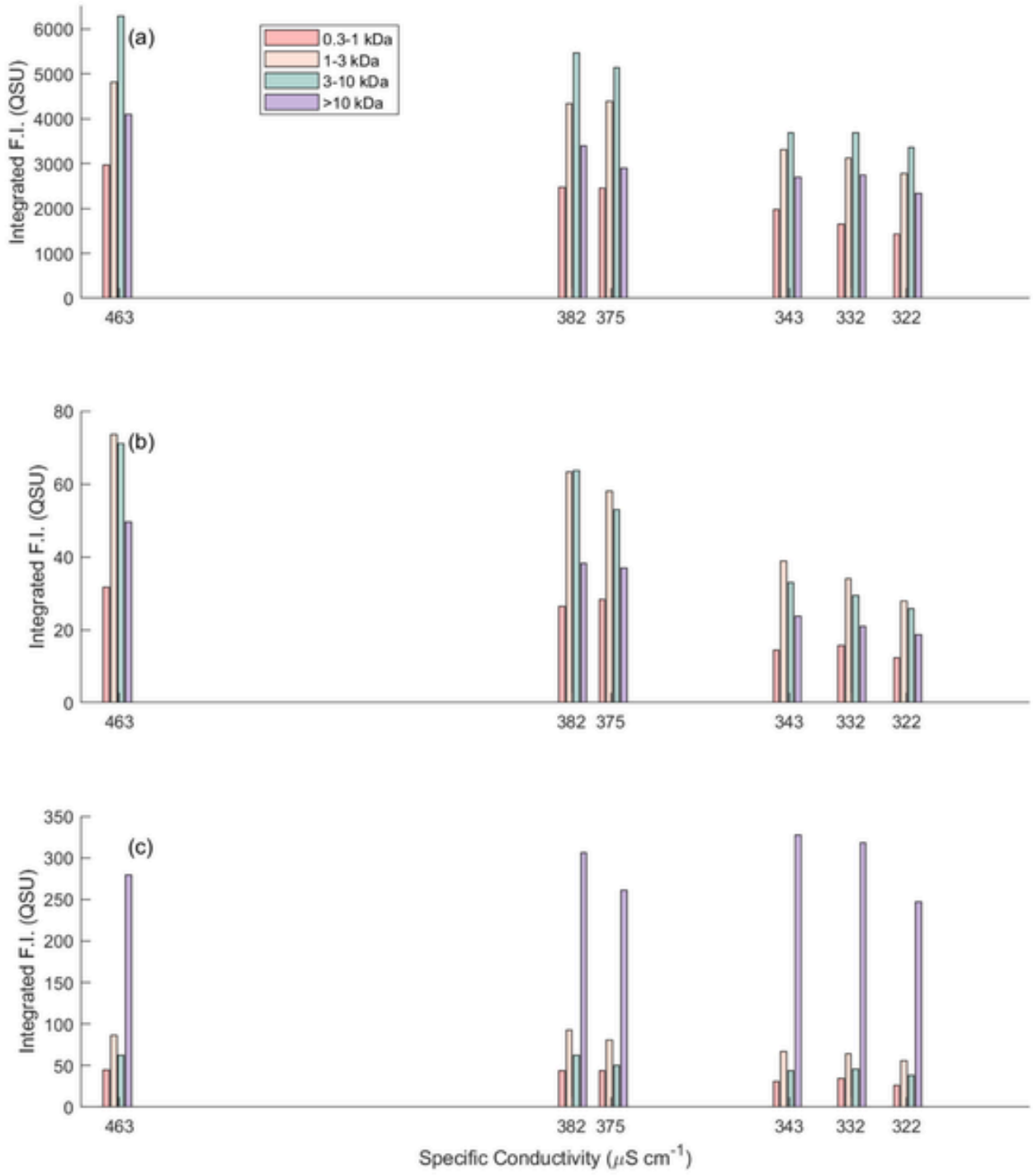

Fig. 3. Molecular weight distributions of different DOM components and their variations with specific conductivity from river water (higher conductivity) to open bay water (lower conductivity) along the lower Fox River-Green Bay ecosystem: (a) UV_{254}, (b) humic-like $Fluor_{350/450}$ (c) protein-like $Fluor_{275/340}$. The four different size fractions, including the 0.3–1 kDa, 1–3 kDa, 3–10 kDa and > 10 kDa, were integrated from the fractograms analyzed by FlFFF.

all 23 components shown in Fig. 4. The most abundant humic-like component, C_{475}, has an emission maximum at 475 nm and covers Peak A and Peak C areas including UVC and UVA humic-like fluorophores (Stedmon and Bro, 2008). The excitation loadings for C_{475} of all samples were highly similar, while their emission loading maxima varied from 435 nm to 475 nm (Fig. 5b). The second major fluorescent component, C_{410} which overlaid with Peak M and Peak A areas, was also a humic-like component which is ubiquitous in natural waters (Coble et al., 1998; Murphy et al., 2018; Wünsch et al., 2019). C_{475} and C_{410} are highly similar with F_{450} and F_{420} observed in Murphy et al. (2018), which have been reported as ubiquitous components in aquatic environments.

The other two protein-like fluorescent components, C_{320} and C_{290}, are both from autochthonous sources. C_{320} has similar fluorescence characteristics to the tryptophan-like fluorophore (Peak T) detected in other aquatic environments. C_{290} resembles the phenylalanine-like peak (Peak B) in the Em < 300 nm area (Coble et al., 2014; Stedmon et al., 2003; Stedmon and Markager, 2005). It is worth noting that there is a

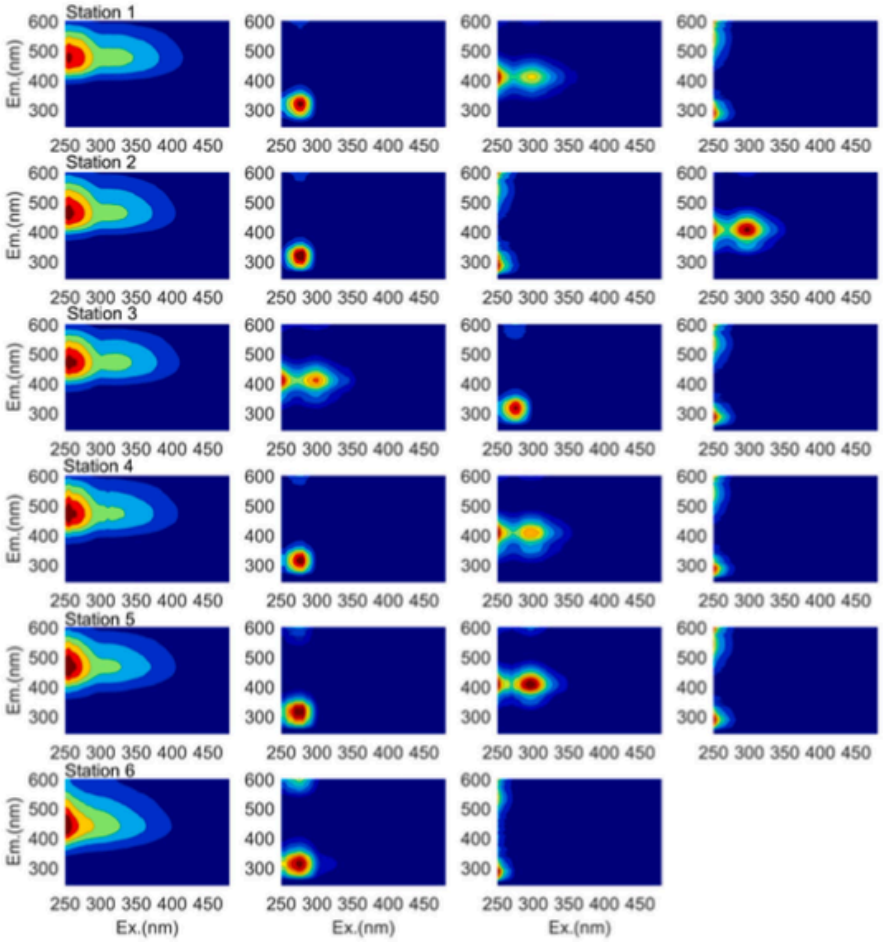

Fig. 4. PARAFAC-derived fluorescent DOM components at each station based on the one sample PARAFAC approach coupling FlFFF size separation and EEM-PARAFAC analysis.

shoulder peak between 400 nm and 600 nm with its maximum at 550 nm shown in the emission loadings of C_{290}. Although this shoulder peak was consistently observed from Station 1 to Station 6, it was at the edge of the 2nd Rayleigh and Raman scattering. This shoulder peak was likely due to artefacts from PARAFAC analysis and needs to be removed during data processing. However, identifying the peak was challenging as C_{290} had weak fluorescence with a high noise/signal ratio.

Based on results from one-sample PARAFAC analysis, variations in fluorescent components, in terms of total fluorescence intensity (ΣF_{max}), and their relative abundance, normalized to total fluorescence intensity (in %), with specific conductivity at stations along the river-bay transect are summarized in Fig. 6.

In general, the fluorescence intensities (ΣF_{max}) of C_{475}, C_{410} and C_{320}, decreased from river water (high conductivity) to bay water (low conductivity), whereas the fluorescence intensity of C_{290} increased along the river-bay transect (Fig. 6a). It is noteworthy that C_{410}, the second abundant humic-like component, was not present at station 6 based on results from the one-sample PARAFAC analysis. As for the relative abundance, a somewhat constant C_{475} abundance, varying between 45 % and 55 % (average of 49.9 ± 4.0 %), was observed along the river-bay transect. The other humic-like component, C_{410}, likely a terrestrial fulvic acid like component (Stedmon et al., 2003; Su et al., 2017), decreased from 36 % at Station 1 to 22 % at Station 5, and disappeared in open Green Bay at Station 6. In contrast, the abundance of C_{320} increased from 11 % in river water to 20 % in open bay water and the C_{290}, also a protein-like component, increased from 4 % to 28 % from river to open Green Bay (Fig. 6b).

4. Discussion

4.1. Estuarine mixing behavior of bulk and size-fractionated DOM

As depicted in Fig. 2, bulk DOM properties, including DOC, DON, CDOM (a_{254}), all show a quasi-conservative mixing behavior during estuarine mixing between Fox River water and open Green Bay water. Accompanying this conservative mixing behavior, other intensive properties (both optical and chemical), such as HIX, $SUVA_{254}$, $S_{275–295}$, E2/E3 and E4/E6 ratios, BIX, and DOC/DON ratio, also monotonically decreased or increased with specific conductivity from river water to open bay water, demonstrating a similar conservative mixing behavior along the river-bay transect. These results pointed to a strong river-dominant DOM source from the Fox River and dynamic changes in DOM chemical properties and composition along the trophic gradient from the lower Fox River to open Green Bay. Similar changes in DOM concentration and composition in other estuarine systems have been reported (Abdulla et al., 2010; Zhou et al., 2016b; Lee and Kim, 2018; Xu et al., 2018b).

In addition to bulk DOM properties, different DOM size-fractions also showed a similar decrease trend in their abundances along the river-bay transect. Based on the variations of DOM concentration in different size-fractions with specific conductivity (Fig. 3), all size-fractions in both bulk CDOM (UV_{254}) and humic-like ($Fluor_{350/450}$) DOM, especially the 1–3 kDa, 3–10 kDa, and > 10 kDa, decreased consistently from river water (high specific conductivity) to open bay water (low specific conductivity), with a significant linear correlation with specific

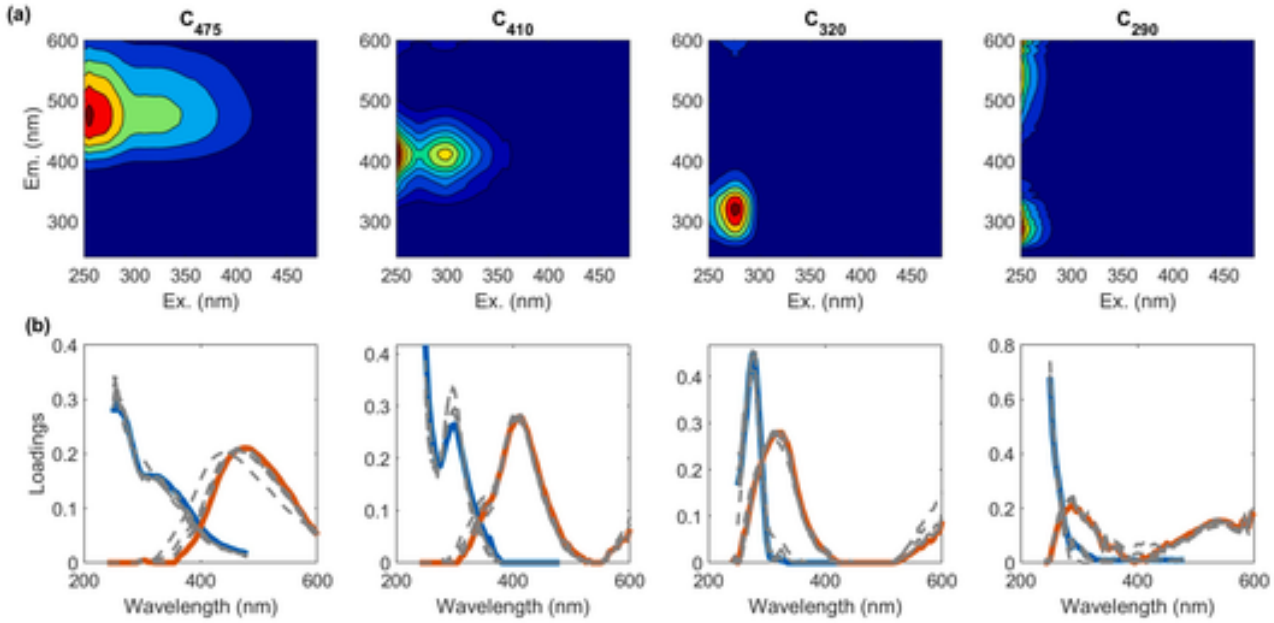

Fig. 5. (a) EEM contours and (b) Excitation/Emission loadings for the four common fluorescent components, C_{475}, C_{410}, C_{320} and C_{290}, identified from the six one-sample PARAFAC models (arranged by Emission wavelengths). The Ex/Em loadings from Station-1 bulk DOM sample were shown in blue line and red line, respectively, while Ex/Em loadings from other stations were plotted in dash grey lines.

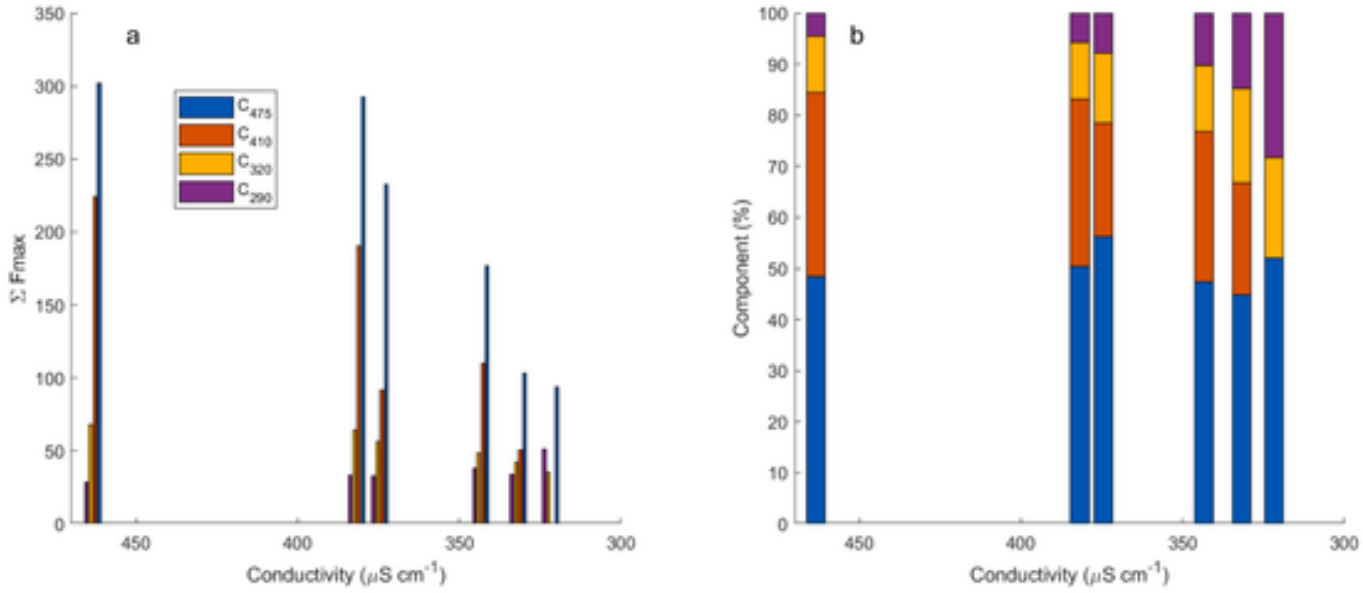

Fig. 6. Variations in (a) fluorescence intensities (ΣF_{max}) and (b) relative abundances (in %) of C_{475}, C_{410}, C_{320} and C_{290} with specific conductivity along the trophic transect in the lower Fox River-Green Bay ecosystem.

conductivity (p-values <0.02). Significant correlations between size-fractionated DOM abundance and specific conductivity are consistent with the variation patterns of a_{254}, HIX and other chemical/optical properties in the whole water samples (Fig. 2). Together, these results indicated that different DOM size-fractions of both UV_{254} and $Fluor_{350/450}$ all had a conservative mixing behavior between river water and bay water. Similar conservative mixing behavior was reported for bulk DOC and CDOM in the study area (DeVillbiss et al., 2016; Xu et al., 2018a) and for humic-like DOM components in a northern Gulf of Mexico estuary (Stolpe et al., 2014; Zhou et al., 2016b).

For the protein-like $Fluor_{275/340}$, there existed no clear variation pattern or concentration gradient for all size-fractions along the river-bay transect (Fig. 3c), showing a non-conservative behavior and sources predominantly from in-situ production or biological processes (Zhou et al., 2016b). Thus, sources of both UV_{254} and $Fluor_{350/450}$ are mostly from river water or terrestrial input in the Green Bay estuary, while the autochthonous DOM components ($Fluor_{275/340}$) partitioned mostly in the >10 kDa size-fraction was predominantly derived from biological processes in the water column.

4.2. Reactivity of different fluorescent components during estuarine mixing

Compared to the classic all-sample PARAFAC analysis, the one-sample PARAFAC approach provided different major fluorescent com-

ponents at each station. For facilitating discussion, the two protein-like fluorescent components, C_{320} and C_{290}, exhibiting similar increase trend from river to open bay, were combined into one autochthonous or aquagenic component. As shown in Fig. 7, the combined autochthonous component increased consistently from river to open Green Bay, which agrees well with the trophic gradient along the river-bay transect and the variation trend of BIX shown in Fig. 2. The abundance of C_{475} remained relatively constant (49.9 ± 4.0 %), showing a seemingly refractory nature during estuarine mixing, consistent with previous studies (Murphy et al., 2018). On the contrast, the relative abundance of C_{410}, a terrestrial fluvic acid-like component (Stedmon et al., 2003; Su et al., 2017), gradually decreased from 36 % in river water (Station 1) to 22 % at Station 5 and become unidentifiable at Station 6 in open Green Bay. Therefore, in contrast to the refractory or persistent nature of C_{475}, component C_{410} could be considered as a semi-labile terrestrial DOM component, which was removed gradually through biological and photochemical processes during its transport along the river-lake transect (Blanchet et al., 2017; Fellman et al., 2010). Thus, the application of one-sample PARAFAC approach provides more compelling results and improves the understanding of DOM heterogeneity and its dynamic changes across hydrological and trophic interfaces in aquatic environments, especially in estuaries. Further studies are needed to provide additional structural and chemical evidence in different DOM size-fractions using available modern analytical techniques (Minor et al., 2014; Lu et al., 2023).

4.3. *Differences in DOM size-distributions between freshwater and marine estuaries*

Compared to the molecular weight distributions of DOM in marine estuaries showing higher colloidal abundances in end-member river water but lower in seawater (Wen et al., 1999; Guo et al., 2009), our results revealed that the >1 kDa colloidal DOM, both DOC and CDOM, in the freshwater estuary is relatively constant (Fig. S1). The difference between freshwater and marine estuaries is largely due to little or no change in salinity or ionic strength in freshwater estuaries. For example, the specific conductivity in Fox River water was 463 μS/cm (salinity 0.3) and 322 μS/cm (salinity 0.2) at station 6 in the open Green Bay with a relatively small change in conductivity between river water and bay water (Table 1). However, the specific conductivity in marine estuaries could increase over 100 times from <300 μS/cm in river water to 50,000 μS/cm in seawater or a salinity change from 0.2 in river water to >30 in seawater, giving rise to coagulation and removal of DOM, especially colloidal DOM, during mixing of river water and seawater in estuaries (Sholkovitz et al., 1978; Guo et al., 2009; Zhou et al., 2016b). Furthermore, the lower Fox River-Green Bay is a negative freshwater estuary with higher conductivity in river water and lower one in lake water (Table 1, Xu et al., 2018a), which should theoretically result in peptization of colloidal DOM and thus a decrease in colloidal DOM abundance during estuarine mixing. However, changes in conductivity or ionic strength seemed too small to result in evidential peptization or changes in colloidal DOM abundances during estuarine mixing in this negative estuary (Fig. 3).

In addition to salinity change, DOM in marine estuaries also suffers from pH change between river water (~7) and seawater (~8.2), resulting in colloidal iron oxide/hydroxide precipitation and the removal of DOM during estuarine mixing (e.g., Sholkovitz et al., 1978; Zhou et al., 2016b) and changes in other biogeochemical processes in estuaries (Yang and Hur, 2014; Lee et al., 2018), all of which affected the size distribution of DOM (Romera-Castillo et al., 2014). In the Fox River estuary, pH changed little between river and bay waters, with an average of 8.9 ± 0.1 (Table 1). Negligible flocculation/aggregation was observed despite both bulk CDOM and humic-like CDOM (represented by $Fluor_{350/450}$) decreased linearly. The relative abundance of each size-fraction remained somewhat unchanged (Fig. 3 and Fig. S5) although there was a small shift in size spectra of the two humic-like components

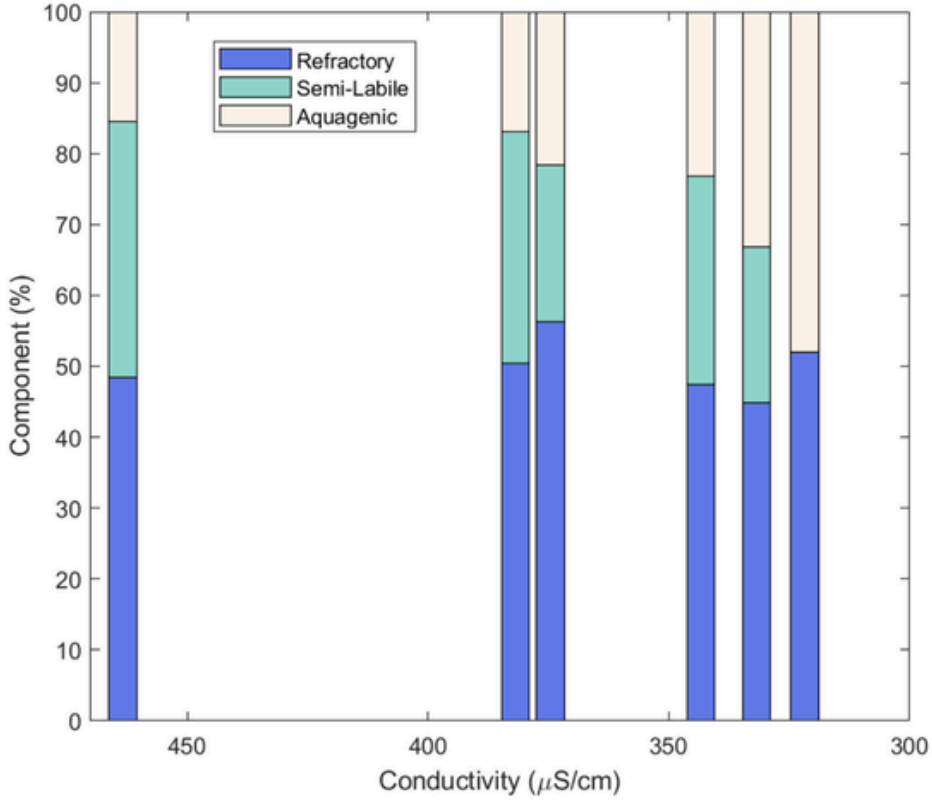

Fig. 7. Variations of fluorescent DOM components along the river-bay transect. "Aquagenic" represents components C_{320} and C_{290}., while "Refractory" represents component C_{475} and "Semi-Labile" represents component C_{410}.

Table 1
Sampling locations, temperature (Temp.), specific conductivity (Sp. Cond.), pH, suspended particulate matter (SPM), and Chlorophyll *a* (Chl-*a*) concentrations for surface waters at each sampling station in the lower Fox River-Green Bay system.

Station	Latitude (°N)	Longitude (°W)	Temp. (°C)	Sp. Cond. (μS/cm)	pH	SPM (mg/L)	Chl-*a* (μg/L)
1	44.52	88.01	26.4	463.4	8.7	28.7	55.18
2	44.54	88.01	26.5	381.8	9.1	33.8	76.90
3	44.56	88.00	25.5	375.8	8.9	26.3	65.86
4	44.60	87.95	24.6	343.4	9.0	12.2	27.23
5	44.65	87.90	24.3	331.8	8.9	5.7	8.54
6	44.72	87.84	23.4	321.8	8.8	4.0	10.68

(C_{475} and C_{410}) at Stations 1–5 (Fig. 8). For example, C_{475} and C_{410} were accumulated and highly overlapped at the 1–10 kDa size interval in spite of their different lability and sources, representing two groups of small heterogeneous humic-like moieties (Her et al., 2003; Romera-Castillo et al., 2014; Wünsch et al., 2017). Thus, our observations partly support the self-assembly hypothesis proposed in previous studies, suggesting that humic substances are comprised of humic-like moieties with similar sizes (Peuravuori and Pihlaja, 2004; Kothawala et al., 2006).

5. Conclusions

The one-sample PARAFAC approach combining FlFFF size-separation and EEM-PARAFAC analysis was utilized to characterize the size distribution of DOM and variations in PARAFAC-derived fluorescent components in a dynamic freshwater estuary in the lower Fox River-Green Bay ecosystem. This approach yielded unique major fluorescent components at each station, with four identified at river/estuarine stations and three at open Green Bay. Based on their sources, composition, and lability, the major fluorescent components were consolidated into three components, namely refractory (represented by humic-like C_{475}) semi-labile (humic-like C_{410}) and labile components (protein-like C_{320} and C_{290}). Throughout the study area, the relative abundances of the refractory component (C_{475}) remained somewhat unchanged. However, the semi-labile component (C_{410}) decreased from river to estuary and eventually vanished in open Green Bay, while the labile components (C_{320} plus C_{290}) increased consistently from river to open Green Bay. These findings offer valuable insights into the dynamic changes in both quantity and quality of bulk DOM along the trophic gradient within the study area and enhance our understanding of the complex biogeochemical processes involved in DOM cycling in the estuarine environment.

CRediT authorship contribution statement

Hui Lin: Sample measurements, Data analysis, Co-writing of the manuscript. **Sarah Bartlett**: Field program, Sample analysis, Review & editing of the manuscript. **Laodong Guo**: Conceptualization, Funding, Co-writing of the manuscript.

All of the authors have approved the final version to publish this paper.

Consent for publication

All authors have approved the manuscript for publication.

Uncited references

Guo and Macdonald, 2006
Guo et al., 2012

Declaration of competing interest

The authors declare no competing interests.

Data availability

The dataset used and/or analyzed during the current study are presented in the manuscript and SI and are available on request.

Acknowledgments

We gratefully thank Bin Yang and the technical staff from NEW Water/Green Bay Metropolitan Sewerage District for their assistance during sample collection, processing, and nutrient analysis. Additionally, we would like to express our appreciation to the Editor and three

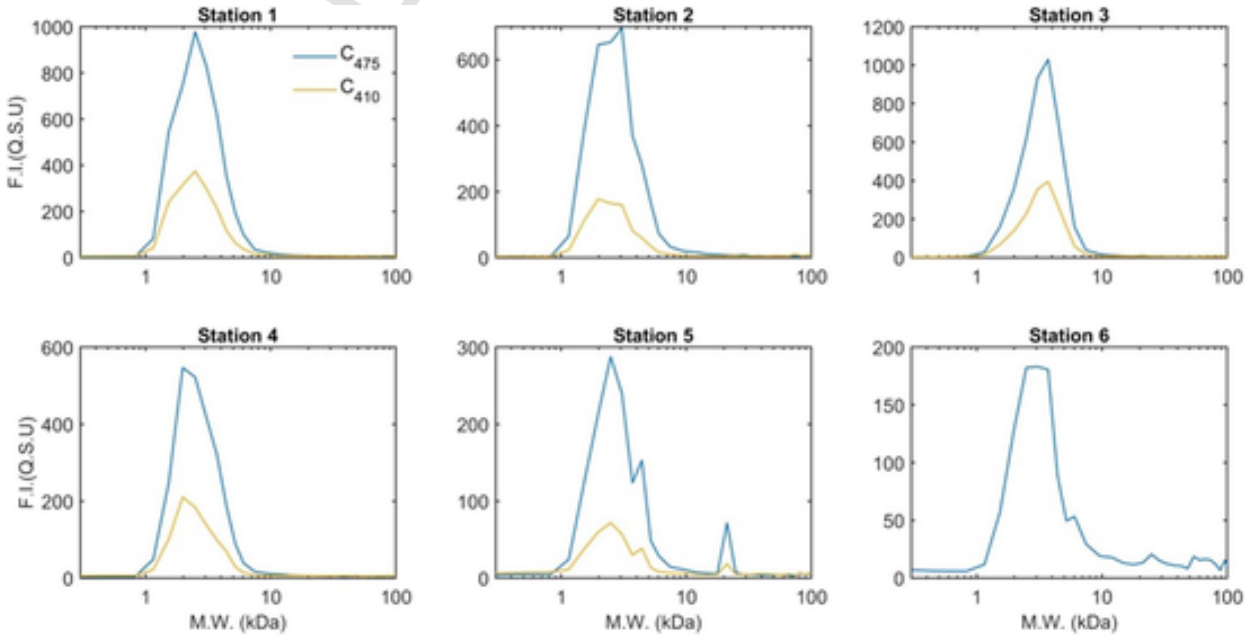

Fig. 8. Size distributions of the two humic-like fluorescence components (C_{475} and C_{410}) at each sampling station in the Fox River-Green Bay ecosystem.

anonymous reviewers for their diligent review and constructive comments. This work was supported in part by Discovery and Innovation *Grant* Program (DIG) from the University of Wisconsin-Milwaukee (101X405 and 101X439) and Freshwater Collaborative of Wisconsin.

Appendix A. Supplementary data

Supplementary data to this article can be found online at https://doi.org/10.1016/j.scitotenv.2023.165891.

References

Abdulla, H.A., Minor, E.C., Dias, R.F., Hatcher, P.G., 2010. Changes in the compound classes of dissolved organic matter along an estuarine transect: a study using FTIR and ^{13}C NMR. Geochim. Cosmochim. Acta 74 (13), 3815–3838.

Aiken, G.R., Hsu-Kim, H., Ryan, J.N., 2011. Influence of dissolved organic matter on the environmental fate of metals, nanoparticles, and colloids. Environ. Sci. Technol. 45, 3196–3201.

Balgooyen, S., Remucal, C.K., 2022. Tributary loading and sediment desorption as sources of PFAS to receiving waters. Acs Es&t Water 2 (3), 436–445.

Bartlett, S.L., Brunner, S.L., Klump, J.V., Houghton, E.M., Miller, T.R., 2018. Spatial analysis of toxic or otherwise bioactive cyanobacterial peptides in Green Bay, Lake Michigan. J. Great Lakes Res. 44 (5), 924–933.

Belzile, C., Guo, L., 2006. Optical properties of low molecular weight and colloidal organic matter: application of the ultrafiltration permeation model to DOM absorption and fluorescence. Mar. Chem. 98 (2–4), 183–196.

Blanchet, M., Fernandez, C., Joux, F., 2017. Photoreactivity of riverine and phytoplanktonic dissolved organic matter and its effects on the dynamics of a bacterial community from the coastal Mediterranean Sea. Prog. Oceanogr. 163, 82–93.

Chen, M., Jaffé, R., 2014. Photo-and bio-reactivity patterns of dissolved organic matter from biomass and soil leachates and surface waters in a subtropical wetland. Water Res. 61, 181–190.

Coble, P.G., 2007. Marine optical biogeochemistry: the chemistry of ocean color. Chem. Rev. 107, 402–418.

Coble, P.G., Del Castillo, C.E., Avril, B., 1998. Distribution and optical properties of CDOM in the Arabian Sea during the 1995 southwest monsoon. Deep-Sea Res. II Topic. Stud. Ocean. 45, 2195–2223. https://doi.org/10.1016/S0967-0645(98)00068-X.

Coble, P.G., Lead, J., Baker, A., Reynolds, D., Spencer, R.G.M., 2014. In: Coble, P.G., Lead, J., Baker, A., Reynolds, D.M., Spencer, R.G.M. (Eds.), Aquatic Organic Matter Fluorescence. 1st ed., Cambridge University Press.

Cole, J.J., Prairie, Y.T., Caraco, N.F., McDowell, W.H., Tranvik, L.J., Striegl, R.G., Duarte, C.M., Kortelainen, P., Downing, J.A., Middelburg, J.J., Melack, J., 2007. Plumbing the global carbon cycle: integrating inland waters into the terrestrial carbon budget. Ecosystems 10, 172–185.

Cuss, C.W., Guéguen, C., 2015. Relationships between molecular weight and fluorescence properties for size-fractionated dissolved organic matter from fresh and aged sources. Water Res. 68, 487–497.

De Haan, H., De Boer, T., 1987. Applicability of light absorbance and fluorescence as measures of concentration and molecular size of dissolved organic carbon in humic Laken Tjeukemeer. Water Res. 21, 731–734.

DeVillbiss, S.E., Zhou, Z., Klump, J.V., Guo, L., 2016. Spatiotemporal variations in the abundance and composition of bulk and chromophoric dissolved organic matter in seasonally hypoxia-influenced Green Bay, Lake Michigan, USA. Sci. Total Environ. 565, 742–757.

Fellman, J.B., Hood, E., Spencer, R.G., 2010. Fluorescence spectroscopy opens new windows into dissolved organic matter dynamics in freshwater ecosystems: a review. Limnol. Oceanogr. 55 (6), 2452–2462.

Guo, L., Macdonald, R.W., 2006. Source and transport of terrigenous organic matter in the upper Yukon River: evidence from isotope ($\delta^{13}C$, $\Delta^{14}C$, and $\delta^{15}N$) composition of dissolved, colloidal, and particulate phases. Glob. Biogeochem. Cycles 20 (2).

Guo, L., Santschi, P.H., 1997. Measurements of dissolved organic carbon (DOC) in sea water by high temperature combustion method. Acta Oceanol. Sin. 16, 339–353.

Guo, L., White, D.M., Xu, C., Santschi, P.H., 2009. Chemical and isotopic composition of high-molecular-weight dissolved organic matter from the Mississippi River plume. Mar. Chem. 114 (3–4), 63–71.

Guo, L., Cai, Y., Belzile, C., Macdonald, R.W., 2012. Sources and export fluxes of inorganic and organic carbon and nutrient species from the seasonally ice-covered Yukon River. Biogeochemistry 107 (1), 187–206.

Helms, J.R., Stubbins, A., Ritchie, J.D., Minor, E.C., Kieber, D.J., Mopper, K., 2008. Absorption spectral slopes and slope ratios as indicators of molecular weight, source, and photobleaching of chromophoric dissolved organic matter. Limnol. Oceanogr. 53, 955–969. https://doi.org/10.4319/lo.2008.53.3.0955.

Her, N., Amy, G., McKnight, D., Sohn, J., Yoon, Y., 2003. Characterization of DOM as a function of MW by fluorescence EEM and HPLC-SEC using UVA, DOC, and fluorescence detection. Water Res. 37 (17), 4295–4303.

Hudson, N., Baker, A., Reynolds, D., 2007. Fluorescence analysis of dissolved organic matter in natural, waste, and polluted waters: a review. River Res. Appl. 23 (6), 631–649.

Huguet, A., Vacher, L., Relexans, S., Saubusse, S., Froidefond, J.M., Parlanti, E., 2009. Properties of fluorescent dissolved organic matter in the Gironde estuary. Org. Geochem. 40, 706–719. https://doi.org/10.1016/j.orggeochem.2009.03.002.

Klump, J.V., Fitzgerald, S.A., Waplesa, J.T., 2009. Benthic biogeochemical cycling, nutrient stoichiometry, and carbon and nitrogen mass balances in a eutrophic freshwater bay. Limnol. Oceanogr. 54, 692–712. https://doi.org/10.4319/lo.2009.54.3.0692.

Klump, J.V., Brunner, S.L., Grunert, B.K., Kaster, J.L., Weckerly, K., Houghton, E.M., Kennedy, J.A., Valenta, T.J., 2018. Evidence of persistent, recurring summertime hypoxia in Green Bay, Lake Michigan. J. Great Lakes Res. 44 (5), 841–850.

Kothawala, D.N., Evans, R.D., Dillon, P.J., 2006. Changes in the molecular weight distribution of dissolved organic carbon within a Precambrian shield stream. Water Resour. Res. 42 (5), W05401.

Lee, M.H., Osburn, C.L., Shin, K.H., Hur, J., 2018. New insight into the applicability of spectroscopic indices for dissolved organic matter (DOM) source discrimination in aquatic systems affected by biogeochemical processes. Water Res. 147, 164–176.

Lee, S.A., Kim, G., 2018. Sources, fluxes, and behaviors of fluorescent dissolved organic matter (FDOM) in the Nakdong River Estuary. Korea. Biogeosciences 15 (4), 1115–1122.

Li, D., Lin, H., Guo, L., 2023. Comparisons in molecular weight distributions and size-dependent optical properties among model and reference natural dissolved organic matter. Environ. Sci. Pollut. Res. 30 (20), 57638–57652.

Lin, H., Guo, L., 2020. Variations in colloidal DOM composition with molecular weight within individual water samples as characterized by flow field-flow fractionation and EEM-PARAFAC analysis. Environ. Sci. Technol. 54, 1657–1667. https://doi.org/10.1021/acs.est.9b07123.

Lin, H., Xu, H., Cai, Y., Belzile, C., Macdonald, R.W., Guo, L., 2021. Dynamic changes in size-fractionated dissolved organic matter composition in a seasonally ice-covered Arctic River. Limnol. Oceanogr. 66 (8), 3085–3099.

Lin, P., Klump, J.V., Guo, L., 2016. Dynamics of dissolved and particulate phosphorus influenced by seasonal hypoxia in Green Bay, Lake Michigan. Sci. Total Environ. 541, 1070–1082. https://doi.org/10.1016/j.scitotenv.2015.09.118.

Lu, K., Xue, J., Guo, L., Liu, Z., 2023. The bio-and thermal lability of dissolved organic matter as revealed by high-resolution mass spectrometry and thermal chemical analyses. Mar. Chem. 250, 104184. https://doi.org/10.1016/j.marchem.2022.104184.

Lu, Y., Bauer, J.E., Canuel, E.A., Yamashita, Y., Chambers, R.M., Jaffé, R., 2013. Photochemical and microbial alteration of dissolved organic matter in temperate headwater streams associated with different land use. J. Geophys. Res. Biogeo. 118, 566–580.

Minor, E.C., Swenson, M.M., Mattson, B.M., Oyler, A.R., 2014. Structural characterization of dissolved organic matter: a review of current techniques for isolation and analysis. Environ Sci Process Impacts 16 (9), 2064–2079.

Modling, R.F., Beeton, A.M., 1970. Dispersal of Fox River water in Green Bay, Lake Michigan. In: Proceedings of the13th Conference on Great Lakes Research. pp. 468–476.

Murphy, K.R., Stedmon, C.A., Graeber, D., Bro, R., 2013. Fluorescence spectroscopy and multi-way techniques. PARAFAC. Analytical Methods 5, 6557–6566.

Murphy, K.R., Timko, S.A., Gonsior, M., Powers, L.C., Wünsch, U.J., Stedmon, C.A., 2018. Photochemistry illuminates ubiquitous organic matter fluorescence spectra. Environ. Sci. Technol. 52, 11243–11250.

Osburn, C.L., Mikan, M.P., Etheridge, J.R., Burchell, M.R., Birgand, F., 2015. Seasonal variation in the quality of dissolved and particulate organic matter exchanged between a salt marsh and its adjacent estuary. J. Geophys. Res. Biogeo. 120 (7), 1430–1449.

Peuravuori, J., Pihlaja, K., 2004. Preliminary study of lake dissolved organic matter in light of nanoscale supramolecular assembly. Environ. Sci. Technol. 38 (22), 5958–5967.

Piccolo, A., Zaccheo, P., Genevini, P.G., 1992. Chemical characterization of humic substances extracted from organic- waste-amended soils. Bio/Technology 40, 275–282.

Robertson, D.M., Hubbard, L.E., Lorenz, D.L., Sullivan, D.J., 2018. A surrogate regression approach for computing continuous loads for the tributary nutrient and sediment monitoring program on the Great Lakes. J. Great Lakes Res. 44 (1), 26–42.

Romera-Castillo, C., Chen, M., Yamashita, Y., Jaffé, R., 2014. Fluorescence characteristics of size-fractionated dissolved organic matter: implications for a molecular assembly based structure? Water Res. 55, 40–51.

Sholkovitz, E.R., Boyle, E.A., Price, N.B., 1978. The removal of dissolved humic acids and iron during estuarine mixing. Earth Planet. Sci. Lett. 40 (1), 130–136.

Stedmon, C.A., Bro, R., 2008. Characterizing dissolved organic matter fluorescence with paral- lel factor analysis: a tutorial. Limnol. Oceanogr. Methods 572–579.

Stedmon, C.A., Markager, S., 2005. Resolving the variability in dissolved organic matter fluorescence in a temperate estuary and its catchment using PARAFAC analysis. Limnol. Oceanogr. 50, 686–697.

Stedmon, C.A., Markager, S., Bro, R., 2003. Tracing dissolved organic matter in aquatic environments using a new approach to fluorescence spectroscopy. Mar. Chem. 82, 239–254.

Stolpe, B., Zhou, Z., Guo, L., Shiller, A.M., 2014. Colloidal size distribution of humic-and protein-like fluorescent organic matter in the northern Gulf of Mexico. Mar. Chem. 164, 25–37.

Su, Y., Hu, E., Feng, M., Zhang, Y., Chen, F., Liu, Z., 2017. Comparison of bacterial growth in response to photodegraded terrestrial chromophoric dissolved organic matter in two lakes. Sci. Total Environ. 579, 1203–1214.

Summers, R.S., Cornel, P.K., Roberts, P.V., 1987. Molecular size distribution and spectroscopic characterization of humic substances. Sci. Total Environ. 62, 27–37.

Weishaar, J.L., Aiken, G.R., Bergamaschi, B.A., Fram, M.S., Fujii, R., Mopper, K., 2003. Evaluation of specific ultraviolet absorbance as an indicator of the chemical composition and reactivity of dissolved organic carbon. Environ. Sci. Technol. 37, 4702–4708. https://doi.org/10.1021/es030360x.

Wen, L.S., Santschi, P., Gill, G., Paternostro, C., 1999. Estuarine trace metal distributions in Galveston Bay: importance of colloidal forms in the speciation of the dissolved phase. Mar. Chem. 63 (3–4), 185–212.
Wünsch, U.J., Murphy, K.R., Stedmon, C.A., 2017. The one-sample PARAFAC approach reveals molecular size distributions of fluorescent components in dissolved organic matter. Environ. Sci. Technol. 51 (20), 11900–11908.
Wünsch, U.J., Stedmon, C.A., Tranvik, L.J., Guillemette, F., 2018. Unraveling the size-dependent optical properties of dissolved organic matter. Limnol. Oceanogr. 63 (2), 588–601.
Wünsch, U.J., Stedmon, C.A., Murphy, K.R., Bro, R., Wenig, P., 2019. Emerging patterns in the global distribution of dissolved organic matter fluorescence. Anal. Methods 11, 888–893.
Xu, H., Guo, L., 2017. Molecular size-dependent abundance and composition of dissolved organic matter in river, lake and sea waters. Water Res. 117, 115–126.
Xu, H., Houghton, E.M., Houghton, C.J., Guo, L., 2018a. Variations in size and composition of colloidal organic matter in a negative freshwater estuary. Sci. Total Environ. 615, 931–941. https://doi.org/10.1016/j.scitotenv.2017.10.019.
Xu, H., Lin, H., Jiang, H., Guo, L., 2018b. Dynamic molecular size transformation of aquatic colloidal organic matter as a function of pH and cations. Water Res. 144, 543–552. https://doi.org/10.1016/j.watres.2018.07.075.
Xu, H., Guan, D.X., Zou, L., Lin, H., Guo, L., 2018c. Contrasting effects of photochemical and microbial degradation on Cu (II) binding with fluorescent DOM from different origins. Environ. Pollut. 23, 205–214.
Yang, B., Lin, H., Bartlett, S.L., Houghton, E.M., Robertson, D.M., Guo, L., 2021. Partitioning and transformation of organic and inorganic phosphorus among dissolved, colloidal and particulate phases in a hypereutrophic freshwater estuary. Water Res. 196, 117025. https://doi.org/10.1016/j.watres.2021.117025.
Yang, L., Hur, J., 2014. Critical evaluation of spectroscopic indices for organic matter source tracing via end member mixing analysis based on two contrasting sources. Water Res. 59, 80–89.
Yang, L., Hur, J., Zhuang, W., 2015. Occurrence and behaviors of fluorescence EEM-PARAFAC components in drinking water and wastewater treatment systems and their applications: a review. Environ. Sci. Pollut. Res. 22 (9), 6500–6510.
Zhao, L., Gao, L., Guo, L., 2021. Seasonal variations in molecular size of chromophoric dissolved organic matter from the lower Changjiang (Yangtze). River. J. Geophys. Res. Biogeosci. 126 (8), e2020JG006160.
Zhou, Z., Guo, L., 2015. A critical evaluation of an asysmmetrical flow field-flow fractionation system for colloidal size characterization of natural organic matter. J. Chromatogr. A 1399, 53–64.
Zhou, Z., Guo, L., Minor, E.C., 2016a. Characterization of bulk and chromophoric dissolved organic matter in the Laurentian Great Lakes during summer 2013. J. Great Lakes Res. 42, 789–801. https://doi.org/10.1016/j.jglr.2016.04.006.
Zhou, Z., Stolpe, B., Guo, L., Shiller, A.M., 2016b. Colloidal size spectra, composition and estuarine mixing behavior of DOM in river and estuarine waters of the northern Gulf of Mexico. Geochim. Cosmochim. Acta 181, 1–17. https://doi.org/10.1016/j.gca.2016.02.032.
Zou, L., Sun, M.Y., Guo, L., 2006. Temporal variations of organic carbon inputs into the upper Yukon River: evidence from fatty acids and their stable carbon isotopic compositions in dissolved, colloidal and particulate phases. Org. Geochem. 37 (8), 944–956.